

# Nitrite Sensor Based on Poly-salicylaldehyde Para-aminobenzoic Acid Film Modified Glassy Carbon Electrode

Yuchun Wang,<sup>1,2\*</sup> Zhaorong Liu,<sup>2</sup> and Chao Tan<sup>1</sup>

<sup>1</sup>Key Lab of Process Analysis and Control of Sichuan Universities, Yibin University, Yibin 644000, Sichuan, China

<sup>2</sup>Department of Applied Chemistry, Yuncheng University, Yuncheng 044000, Shanxi, China

(Received February 15, 2021; accepted April 1, 2021)

**Keywords:** nitrite, poly-salicylaldehyde para-aminobenzoic acid film, modified electrode, sensor

A simple and environmentally friendly electrochemical deposition method was used to prepare a poly-salicylaldehyde para-aminobenzoic acid modified glassy carbon electrode (poly-SAPABA GCE), and an electrochemical sensor for the detection of nitrite was successfully constructed. The electrochemical performance of the poly-SAPABA GCE was investigated by electrochemical impedance spectroscopy, chronocoulometry, and cyclic voltammetry (CV). The results showed that the poly-SAPABA film promoted electron transfer, which improved the electrochemical performance. The poly-SAPABA GCE has a good electrocatalytic performance for the detection of nitrite. The CV curves for the poly-SAPABA GCE were measured in pH 3.25 phosphate buffered solution (PBS) containing nitrite. The peak current of nitrite increased linearly with the nitrite concentration in the range from  $3.12 \times 10^{-5}$  to  $1.53 \times 10^{-2}$  mol L<sup>-1</sup> with a correlation coefficient of 0.9999, and a detection limit of  $5.04 \times 10^{-6}$  mol L<sup>-1</sup> at a signal-to-noise ratio of 3 was calculated. The poly-SAPABA GCE also has good selectivity, stability, and reproducibility, and was successfully applied to the determination of nitrite in actual samples. The recovery of nitrite was 96–105% and the relative standard deviation was 3.28%. The proposed method can potentially be used for the detection of nitrite.

## 1. Introduction

Nitrite is a color former that is allowed to be used in limited amounts in meat products. However, nitrite poisoning has often occurred from the consumption of pickled meat products and pickles.<sup>(1)</sup> In addition, by drinking bitter well water and distilled water containing nitrite, nitrite enters the blood and oxidizes oxygen-carrying hypohemoglobin to methemoglobin, thus causing tissue hypoxia and poisoning owing to reduced oxygen-carrying capacity.<sup>(2)</sup> Therefore, the detection of nitrite has practical importance. There are many nitrite detection methods, including spectrometry,<sup>(3)</sup> colorimetric detection,<sup>(4,5)</sup> fluorescence detection,<sup>(6,7)</sup> and chemiluminescence.<sup>(8)</sup> Although these methods have high sensitivity and accurate detection, it is difficult to realize online on-site detection due to cumbersome sample processing and the use of large and expensive precision instruments. Therefore, their use is limited. However, an electrochemical sensor has the advantages of convenient operation and portability, making it

---

\*Corresponding author: e-mail: wyc0104@126.com  
<https://doi.org/10.18494/SAM.2021.3335>

easier to realize real-time detection in the field. Mejri *et al.*<sup>(9)</sup> constructed a non-enzymatic sensor based on a curcumin-modified pencil graphite electrode loaded with molybdenum disulfide nanosheet decorated gold foam. The sensor was used to analyze spiked samples of river water and industrial wastewater with excellent reproducibility and stability. Luo *et al.*<sup>(10)</sup> developed effective, fast, and highly selective nanogold film interdigital electrode sensors that can detect nitrite easily and quickly. However, these sensors use the expensive metal gold and are cumbersome to build. A Schiff base is formed by the condensation of para-aminobenzoic acid and salicylaldehyde. Schiff bases are compounds bearing an imine group with a carbon–nitrogen double bond, generally with the nitrogen atom bonded to an alkyl or aryl group. They are easy to prepare, they have versatile steric and electronic properties, and the suitable choice of amines and substituents on the aromatic rings can provide modified electrodes with the desired features. Teixeira *et al.*<sup>(11)</sup> determined dipyrone concentration in pharmaceutical formulations using a carbon electrode chemically modified with a Schiff base, more specifically, a carbon paste electrode modified with an *N,N'*-ethylenebis(salicylideneiminato)oxovanadium(IV) Schiff base complex. In this study, on the basis of previous research on polymer-modified electrodes,<sup>(12–14)</sup> a poly-salicylaldehyde para-aminobenzoic acid modified glassy carbon electrode (poly-SAPABA GCE) was developed with good electrocatalytic performance for the detection of nitrite. Owing to its advantages of a simple preparation procedure, good stability, high reliability, and low cost, it is a highly promising electrochemical sensor for detecting nitrite.

## 2. Experimental Methods

### 2.1 Chemicals

Salicylaldehyde and para-aminobenzoic acid were purchased from Tianjin Damao Chemical Reagent Factory. Sodium nitrite was purchased from Tianjin Standard Technology Co. Ltd. The concentrated  $\text{H}_2\text{SO}_4$ , concentrated  $\text{HNO}_3$ , KCl, NaOH,  $\text{KH}_2\text{PO}_4$ , and  $\text{K}_2\text{HPO}_4$  used as reagents were of analytical grade and used without further purification.

### 2.2 Apparatus

All the electrochemical measurements were carried out on a CHI660C electrochemical workstation (Chenhua Instrument Co. Ltd.). A conventional three-electrode system comprising a glass carbon electrode ( $\phi = 4$  mm, GCE) or poly-SAPABA GCE as the working electrode, a platinum counter electrode, and a saturated calomel electrode as a reference was used. A KQ3200E numerical control ultrasonic wave cleaner was purchased from Ultrasonic Instrument Co. Ltd. (Kunshan). A pH meter (PHS-3C, Shanghai Dapu Instrument Co. Ltd.) and a BS110S electronic balance (Shanghai Jingsheng Scientific Instrument Co. Ltd.) were also used.

### 2.3 Preparation of poly-SAPABA GCE

Before the preparation, the GCE was cleaned by polishing with metallographic sandpaper, immersing in 1:1 nitric acid for 5 min with ultrasonic cleaning, immersing in absolute ethyl

alcohol for 5 min with ultrasonic cleaning, rinsing in deionized water for 3 min, and allowing to air dry. After pretreatment, the cleaned GCE was placed in  $0.5 \text{ mol L}^{-1}$  sulfuric acid, then cyclic voltammetry (CV) experiments were carried out from  $-1.0$  to  $1.0 \text{ V}$  with a scan rate of  $0.10 \text{ V s}^{-1}$  until the peak current remained stable, thus attaining an activation electrode. Next, a poly-SAPABA film was deposited on the GCE using CV by setting potential limits of  $-1.0$  to  $1.0 \text{ V}$  over 15 cycles at a scan rate of  $0.05 \text{ V s}^{-1}$  in an electrolyte solution containing  $0.1 \text{ mol L}^{-1}$  potassium chloride,  $1.0 \text{ mol L}^{-1}$  sodium hydroxide,  $5.02 \times 10^{-3} \text{ mol L}^{-1}$  salicylaldehyde, and para-aminobenzoic acid. The synthesized poly-SAPABA GCE electrode was then removed, rinsed, and dried in air. A light yellow film was observed on the surface of the electrode, indicating the successful preparation of a stable poly-SAPABA GCE.

## 2.4 Experimental methods

All electrochemical measurements were performed at room temperature and nitrogen was bubbled into the sample to remove the oxygen. A conventional three-electrode system was employed using the CHI660C electrochemical workstation. Electrochemical impedance spectroscopy (EIS) was performed with  $1.01 \times 10^{-3} \text{ mol L}^{-1} \text{ K}_3[\text{Fe}(\text{CN})_6]$  as a probe, an electric potential of  $0.01 \text{ V}$ , a frequency range from  $0.01$  to  $10^5 \text{ Hz}$ , and a sinusoidal voltage with an amplitude of  $5 \text{ mV}$ . Double-potential-step Coulomb analysis was performed in the electric potential range from  $-0.4$  to  $0.7 \text{ V}$  with a pulse width of  $0.25 \text{ s}$ , a sample interval of  $2.5 \times 10^{-4} \text{ s}$ , and a  $\text{NO}_2^-$  concentration of  $1.04 \times 10^{-3} \text{ mol L}^{-1}$ . CV curves were recorded from  $0$  to  $1.2 \text{ V}$  for various scan rates, pH values of the electrolyte, and  $\text{NO}_2^-$  concentrations.

## 3. Results and Discussion

### 3.1 Electrochemical performance of poly-SAPABA GCE

To evaluate the electrochemical performance and interfacial properties of the electrodes, EIS was performed in the frequency range of  $0.01$  to  $10^5 \text{ Hz}$ , as shown in Fig. 1, with  $1.01 \times 10^{-3}$

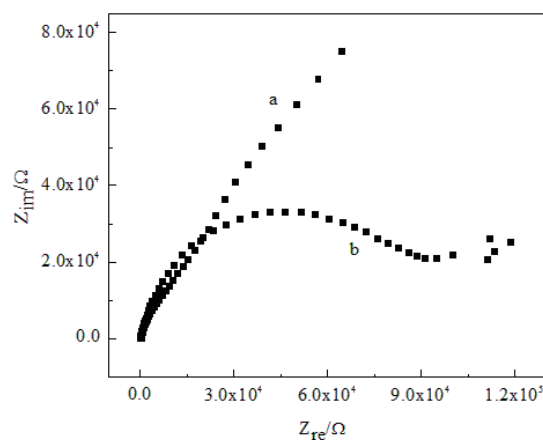


Fig. 1. EIS curves of (a) poly-SAPABA GCE and (b) bare GCE in  $0.1 \text{ mol L}^{-1} \text{ KCl}$  containing  $1.01 \times 10^{-3} \text{ mol L}^{-1} \text{ K}_3[\text{Fe}(\text{CN})_6]$ .

$\text{mol L}^{-1} \text{K}_3[\text{Fe}(\text{CN})_6]$  used as a probe and the poly-SAPABA GCE (a) and GCE (b) used as the working electrode. In EIS spectra, the semicircular portion in the high-frequency region represents the electron-transfer resistance ( $R_{\text{et}}$ ) of the electrode, and the linear tail at lower frequencies indicates the diffusion-limited process.<sup>(15)</sup> As shown in Fig. 1, a large semicircle appeared for the bare GCE (curve b) because of the high  $R_{\text{et}}$ . After the GCE was modified with the poly-SAPABA film, the semicircle nearly disappeared and an almost linear relation was observed, which implies that the  $R_{\text{et}}$  of the poly-SAPABA GCE electrode surface decreased and the charge transfer rate increased. Therefore, the poly-SAPABA film can promote electron transfer from the electroactive markers to the modified electrode surface.<sup>(16)</sup>

Figure 2 shows chronocoulometry curves of the double-potential step of the poly-SAPABA GCE (a) and bare GCE (b) in PBS solution (pH = 3.25) containing  $1.04 \times 10^{-3} \text{ mol L}^{-1} \text{NO}_2^-$ . For both the forward potential step and the reverse potential step, the charge reaches a maximum in a very short time, indicating that the forward and reverse reaction rates are very high and the conversion between the oxidizer and reducer on the electrode surface is very fast.<sup>(17)</sup> Figure 2 also shows a gentle change in the charge on the bare GCE (curve b), and the maximum charge is much less than that on the poly-SAPABA GCE (curve a). Hence, less electricity per unit time is passed on the bare GCE than on the poly-SAPABA GCE. It has thus been further confirmed that the poly-SAPABA film facilitates electron transfer.

The CV curves were measured on the poly-SAPABA GCE (curve a') and GCE (curve b') in the pH 3.25 PBS solution (Fig. 3) and no peaks were observed. The area under CV curve a' is greater than that under CV curve b'. The results showed that the poly-SAPABA film was successfully electrically polymerized on the bare GCE, and the capacitance current of the poly-SAPABA GCE was significantly increased. Thus, the chronocoulometry and CV results confirmed that the poly-SAPABA film promoted electron transfer and exhibited favorable electrochemical performance.

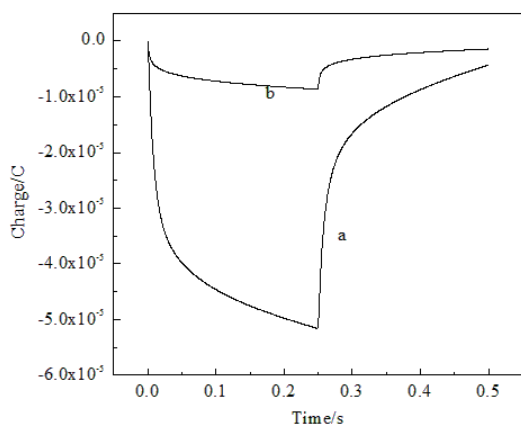


Fig. 2. Chronocoulometry curves of double-potential step of poly-SAPABA GCE (a) and bare GCE (b) in PBS solution (pH = 3.25) containing  $1.04 \times 10^{-3} \text{ mol L}^{-1} \text{NO}_2^-$ .

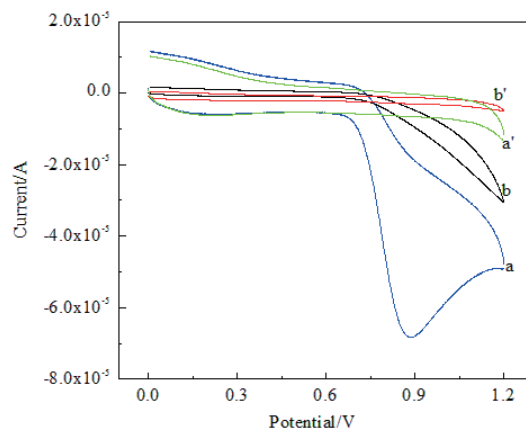


Fig. 3. (Color online) CV curves of poly-SAPABA GCE (a and a') and bare GCE (b and b') in the presence of  $0 \text{ mol L}^{-1}$  (a' and b') and  $1.04 \times 10^{-3} \text{ mol L}^{-1} \text{NO}_2^-$  (a and b) in pH 3.25 PBS with potential ranging from 0 to 1.20 V at a scan rate of 0.12 V/s.

### 3.2 Electrochemical response and behavior of nitrite at poly-SAPABA GCE

#### 3.2.1 Electrocatalytic property

The CV curves were measured with a scan rate of  $0.12 \text{ V s}^{-1}$  on the poly-SAPABA GCE (curve a) and GCE (curve b) in the pH 3.25 PBS solution containing  $1.04 \times 10^{-3} \text{ mol L}^{-1} \text{ NO}_2^-$ , as shown in Fig. 3. There is a broad peak and the peak current is small at the bare GCE, indicating that the effectiveness of electrochemical detection for  $\text{NO}_2^-$  is poor. A significant oxidation peak is observed on the poly-SAPABA GCE. It is thus shown that the poly-SAPABA film provides more electroactive sites for the oxidation of  $\text{NO}_2^-$  and accelerates the electron transfer. Figure 3 suggests the good electrochemical properties and fast electron transfer of the poly-SAPABA GCE.

#### 3.2.2 Optimization of sensor

The pH of the electrolyte solution directly affects the sensitivity of the electrochemical determination of  $\text{NO}_2^-$ . Thus, the effect of the pH on the electrocatalytic oxidation of sodium nitrite by the poly-SAPABA GCE in solutions with pH values of 1.17, 2.62, 3.25, 4.51, 5.58, 5.66, and 7.01 was investigated. Figure 4 shows the CV curves obtained at a scan rate of  $0.12 \text{ V s}^{-1}$  in different pH PBS solutions containing  $1.04 \times 10^{-3} \text{ mol L}^{-1} \text{ NO}_2^-$ . The results clearly show that the peak current increases until pH 3.25 and then gradually decreases. At higher pH values, as the current decreases, the peak potential increases and the peak shape also changes. Hence, pH 3.25 was considered to be the optimum value for the determination of sodium nitrite.

Moreover, the effect of the scan rate (0.08, 0.10, 0.12, 0.15, 0.18, 0.22, 0.26, 0.30, and  $0.34 \text{ V s}^{-1}$ ) on the CV response of the poly-SAPABA GCE in the PBS solution (pH = 3.25) containing  $1.04 \times 10^{-3} \text{ mol L}^{-1} \text{ NO}_2^-$  was investigated. As displayed in the inset of Fig. 5, both

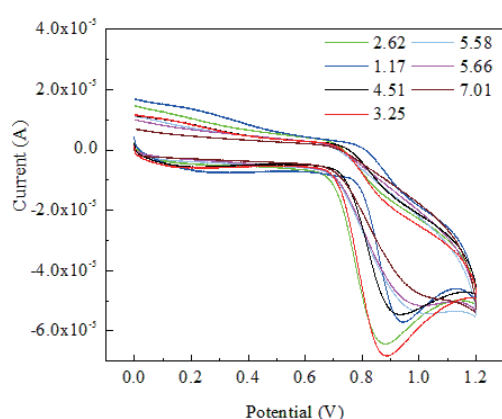


Fig. 4. (Color online) CV curves of  $1.04 \times 10^{-3} \text{ mol L}^{-1} \text{ NO}_2^-$  on poly-SAPABA GCE in PBS solution with various pH values.

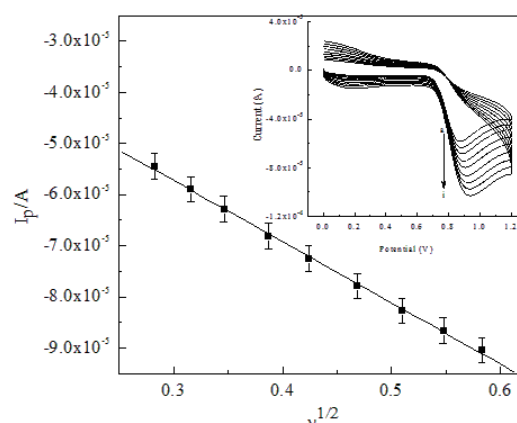


Fig. 5. Relationship between peak current and square root of scan rate. The inset shows CV curves of  $1.04 \times 10^{-3} \text{ mol L}^{-1} \text{ NO}_2^-$  on the poly-SAPABA GCE in PBS solution of pH 3.25 with scan rates of (a) 0.08, (b) 0.10, (c) 0.12, (d) 0.15, (e) 0.18, (f) 0.22, (g) 0.26, (h) 0.30, and (i)  $0.34 \text{ V s}^{-1}$ .

the peak current and the peak potential increased with increasing scan rate. The peak potential shifted from 0.872 V at a scan rate of  $0.08 \text{ V s}^{-1}$  to 0.924 V at a scan rate of  $0.34 \text{ V s}^{-1}$ , indicating that  $\text{NO}_2^-$  electrocatalytic oxidation on the poly-SAPABA GCE is an irreversible process. The peak current ( $I_p$ ) exhibited a linear dependence on the square root of the scan rate ( $v^{1/2}$ ) from 0.08 to  $0.34 \text{ V s}^{-1}$ , as shown in Fig. 5, and the calibration equation can be expressed as  $I_p = -1.199 \times 10^{-4} v^{1/2} - 2.126 \times 10^{-5}$  ( $R^2 = 0.9993$ ), which indicates that the catalytic oxidation of nitrite on the poly-SAPABA GCE is a diffusion-limited process in the range of the scan rate.<sup>(18)</sup>

### 3.3 Determination of nitrite at poly-SAPABA GCE

The determination of nitrite at different concentrations in the pH 3.25 PBS solution at the poly-SAPABA GCE was studied at a scan rate of  $0.12 \text{ V s}^{-1}$ , and the CV curves are shown in the inset of Fig. 6. The peak current of nitrite increased proportionally with increasing nitrite concentration in the range from  $3.12 \times 10^{-5}$  to  $1.53 \times 10^{-2} \text{ mol L}^{-1}$  (Fig. 6). The linear regression equation is  $I_p \text{ (A)} = -0.0420 C \text{ (mol L}^{-1}) - 3.170 \times 10^{-6}$  ( $R^2 = 0.9999$ ). A detection limit of  $5.04 \times 10^{-6} \text{ mol L}^{-1}$  at a signal-to-noise ratio of 3 was calculated.

### 3.4 Reproducibility, stability, and selectivity

The reproducibility of the proposed sensor for nitrite determination was studied under optimal experimental conditions. Five repeated measurements were performed for  $1.04 \times 10^{-3} \text{ mol L}^{-1} \text{ NO}_2^-$  using the same poly-SAPABA GCE. The relative standard deviation (RSD) of the peak current was 2.23%. For the same solution containing nitrite, three different poly-SAPABA GCEs were prepared and used for measurement, and the RSD of the measurement was calculated to be 3.66%. These results confirm that the poly-SAPABA GCE has excellent reproducibility.

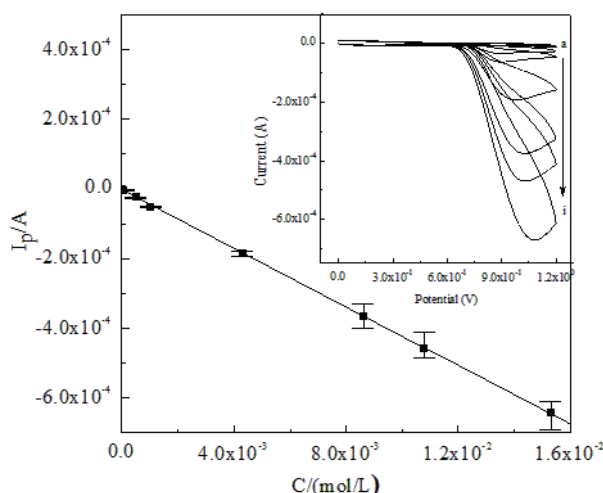


Fig. 6. Relationship between peak current and concentration of  $\text{NO}_2^-$ . The inset shows CV curves for  $\text{NO}_2^-$  concentrations of (a)  $3.12 \times 10^{-5}$ , (b)  $5.07 \times 10^{-5}$ , (c)  $8.30 \times 10^{-5}$ , (d)  $5.20 \times 10^{-4}$ , (e)  $1.04 \times 10^{-3}$ , (f)  $4.32 \times 10^{-3}$ , (g)  $8.64 \times 10^{-3}$ , (h)  $1.08 \times 10^{-2}$ , and (i)  $1.53 \times 10^{-2} \text{ mol L}^{-1}$ .

Then the poly-SAPABA GCE was rinsed and kept in the PBS solution (pH = 3.25). The storage stability of the designed nitrite sensor was investigated. For the detection of  $1.04 \times 10^{-3}$  mol L<sup>-1</sup> NO<sub>2</sub><sup>-</sup>, there was no decrease in the current response in the first 3 days or significant decrease in the current response after a week, with the peak current still at 99.3% of its original value. Moreover, after 3 weeks, the peak current was still at 97.4% of its original value. These results indicate that the stability of the poly-SAPABA GCE is sufficient for the continuous detection of nitrite.

The anti-interference ability of the electrode is very important for actual sample detection. The possibility of interference in the electrochemical detection of nitrite at the poly-SAPABA GCE was examined by adding various foreign species to the PBS solution (pH = 3.25) containing  $1.04 \times 10^{-3}$  mol L<sup>-1</sup> of nitrite. There was no change in the peak current when various common cations and anions were added with a concentration of 500 times the NO<sub>2</sub><sup>-</sup> concentration, as shown in Table 1. The results reveal that the sensor has strong anti-interference ability for the detection of nitrite.

### 3.5 Analysis of real samples

To assess the feasibility of the proposed sensor for practical application, the concentration of nitrite in water samples was detected through a standard addition method. Industrial wastewater was allowed to stand for at least 1 day before use, then the supernatant liquid was substituted for distilled water to prepare the PBS solution (pH = 3.25). A recovery experiment in which  $1 \times 10^{-5}$  mol L<sup>-1</sup> NO<sub>2</sub><sup>-</sup> was added was carried out and the recovery was determined three times. The results are listed in Table 2 and show that the recovery of NO<sub>2</sub><sup>-</sup> in the industrial wastewater was 96–105% with an RSD of 3.28%. In addition, to confirm the accuracy of the proposed method, spectrophotometry<sup>(19)</sup> was applied to detect the original samples, and the results were consistent with those of our proposed method. Therefore, the proposed sensor can be used to detect the concentration of nitrite.

Table 1  
Peak current upon the addition of different interference ions.

Interfering ion	None	Cl <sup>-</sup>	SO <sub>4</sub> <sup>2-</sup>	CO <sub>3</sub> <sup>2-</sup>	NO <sub>3</sub> <sup>-</sup>	Al <sup>3+</sup>	Mg <sup>2+</sup>	K <sup>+</sup>	Zn <sup>2+</sup>	Ca <sup>2+</sup>	NH <sub>4</sub> <sup>+</sup>
Peak current (×10 <sup>-5</sup> A)	-5.224	-5.221	-5.222	-5.226	-5.224	-5.225	-5.220	-5.221	-5.223	-5.226	-5.223

Table 2  
Analytical results for the determination of nitrite in samples.

Industrial wastewater	Spectrophotometry (mol L <sup>-1</sup> )	Original (mol L <sup>-1</sup> )	Added (mol L <sup>-1</sup> )	Total found (mol L <sup>-1</sup> )	Recovery (%)
Sample 1	$5.38 \times 10^{-5}$	$5.31 \times 10^{-5}$	$1 \times 10^{-5}$	$6.36 \times 10^{-5}$	105
Sample 2	$5.29 \times 10^{-5}$	$5.33 \times 10^{-5}$	$1 \times 10^{-5}$	$6.32 \times 10^{-5}$	99
Sample 3	$5.32 \times 10^{-6}$	$5.39 \times 10^{-5}$	$1 \times 10^{-5}$	$6.35 \times 10^{-5}$	96



## 4. Conclusions

In this research, we developed a low-cost electrochemical sensor with a poly-SAPABA GCE using electrochemical deposition technology. Electrochemical studies revealed that the as-synthesized poly-SAPABA film shows high electrical conductivity, a good rate of electron transfer, and excellent electrocatalytic activity toward the oxidation of nitrite, providing an effective, rapid, and high-specificity method for the detection of nitrite in water, which is suitable for real-time applications.

## Acknowledgments

The authors are grateful for the financial support from the Open Foundation of Key Lab of Process Analysis and Control of Sichuan Universities (Yibin University Grant No. 2019004), the Doctor Research Fund of Yuncheng University (YQ-2019024), and the Applied Basic Research Programs of Foundation of Yuncheng University (CY-2019032).

## References

- 1 H. Le, D. Tran, N. Kim, and J. Lee: *J. Colloid Interface Sci.* **583** (2021) 425. <https://doi.org/10.1016/j.jcis.2020.09.068>
- 2 S. Wang, Q. Lin, S. Filbrun, R. Zhou, Q. An, Y. Yin, W. Xu, D. Xu, and C. Liu: *Sens. Actuators, B* **328** (2021) 129073. <https://doi.org/10.1016/j.snb.2020.129073>
- 3 N. Altunay and A. Elik: *Food Chem.* **332** (2020) 127395. <https://doi.org/10.1016/j.foodchem.2020.127395>
- 4 T. Thongkam and K. Hemavibool: *Microchem. J.* **159** (2020) 105412. <https://doi.org/10.1016/j.microc.2020.105412>
- 5 O. Adegoke, S. Zolotovskaya, A. Abdolvand, and N. Daeid: *Talanta* **224** (2021) 121875. <https://doi.org/10.1016/j.talanta.2020.121875>
- 6 K. Yu, S. Pan, K. Li, L. Shi, Y. Liu, S. Chen, and X. Yu: *Food Chem.* **341** (2021) 128254. <https://doi.org/10.1016/j.foodchem.2020.128254>
- 7 B. Li, Y. Li, and X. Gao: *Food Chem.* **274** (2019) 162. <https://doi.org/10.1016/j.foodchem.2018.08.112>
- 8 J. Wu, X. Wang, Y. Lin, Y. Zheng, and J. Lin: *Talanta* **154** (2016) 73. <https://doi.org/10.1016/j.talanta.2016.03.062>
- 9 A. Mejri, A. Mars, H. Elfil, and A. Hamzaoui: *Anal. Chim. Acta.* **1137** (2020) 19. <https://doi.org/10.1016/j.aca.2020.08.032>
- 10 H. Luo, X. Lin, Z. Peng, Y. Zhou, S. Xu, M. Song, L. Jin, and X. Zheng: *Frontiers Chem.* **8** (2020) 366. <https://doi.org/10.3389/fchem.2020.00366>
- 11 M. Teixeira, L. Marcolino-Junior, O. Fatibello-Filho, E. Dockal, and É. Cavalheiro: *J. Brazil. Chem. Soc.* **15** (2004) 803. <https://www.researchgate.net/publication/233860418>
- 12 Z. Liu, Y. Wang, and Q. Gong: *Chin. J. Anal. Chem.* **38** (2010) 1040. <https://kns.cnki.net/KCMS/detail/detail.aspx?dbcode=CJFQ&dbname=CJFD2010&filename=FXHX201007036&v=MjA0OTVUcldNMUZyQ1VSN3VmWmVkc0Z5emxWYjdCSXpYRGRyRzRIOUhNcUk5R1lvUjhlWDFMdXhZUzdEaDFUM3E=>
- 13 H. Han, Q. Gong, J. Qin, Y. Wang, and C. Yao: *J. Anal. Sci.* **34** (2018) 249. <https://kns.cnki.net/KCMS/detail/detail.aspx?dbcode=CJFQ&dbname=CJFDLAST2018&filename=FXKX201802022&v=MjkxNzFNclK5SFpvUjhlWDFMdXhZUzdEaDFUM3FUcldNMUZyQ1VSN3VmWmVkc0Z5emxXcjdPSXpYQWRyRzRIOW4=>
- 14 Z. Liu, Y. Wang, and C. Tan: *Sens. Mater.* **32** (2020) 3273. <https://doi.org/10.18494/SAM.2020.2872>
- 15 Y. Ge, F. Gu, L. Liu, P. Fang, J. Zhou, H. Cheng, J. Ma, Z. Tong, J. Wang, and B. Zhang: *J. Mater. Res.* **35** (2020) 1. <https://doi.org/10.1557/jmr.2020.225>
- 16 G.-M. Masoud and T. Mohammad Ali: *Biosens. Bioelectron.* **109** (2018) 279. <https://doi.org/10.1016/j.bios.2018.02.057>
- 17 W. Jiang, L. Huang, and Y. Zhong: *Chin. J. Anal. Chem.* **39** (2011) 1038. <https://kns.cnki.net/KCMS/detail/detail.aspx?dbcode=CJFQ&dbname=CJFD2011&filename=FXHX201107020&v=MTE2OTBkc0Z5emxXcJNBSXpYRGRyRzRIOURNcUk5SFpUjhlWDFMdXhZUzdEaDFUM3FUcldNMUZyQ1VSN3VmWmU=>
- 18 J.-M. Jian, L. Fu, J. Ji, L. Lin, X. Guo, and T.-L. Ren: *Sens. Actuators, B* **262** (2018) 125. <https://doi.org/10.1016/j.snb.2018.01.164>



- 19 W. Yuan, Y. Zhang, and C. Zhao: *Phy. Chem. Exam.* **50** (2014) 383. <https://kns.cnki.net/kcms/detail/detail.aspx?dbcode=CJFD&dbname=CJFD2014&filename=LHJH201403036&v=7t4KiCHJyisOCsW3LiOgZ5NzROoJrz4JgXOhZbtGwHgoQ0aLmvARVCdfDV7BRPWH>

